Journal Pre-proof

Disruption of tuftelin 1, a desmosome associated protein, causes skin fragility, woolly hair and palmoplantar keratoderma

Annemieke J.M.H. Verkerk, Daniela Andrei, Mathilde C.S.C. Vermeer, Duco Kramer, Marloes Schouten, Pascal Arp, Joost A.M. Verlouw, Hendri H. Pas, Hillegonda J. Meijer, Marije van der Molen, Silke Oberdorf-Maass, Miranda Nijenhuis, Pedro H. Romero-Herrera, Martijn F. Hoes, Jeroen Bremer, Johan A. Slotman, Peter C. van den Akker, Gilles F.H. Diercks, Ben N.G. Giepmans, Hans Stoop, Jasper Saris, Ans M.W. van den Ouweland, Rob Willemsen, Jean-Jacques Hublin, M. Christopher Dean, A. Jeannette M. Hoogeboom, Herman H.W. Silljé, André G. Uitterlinden, Peter van der Meer, Maria C. Bolling

PII: S0022-202X(23)02581-2

DOI: https://doi.org/10.1016/j.jid.2023.02.044

Reference: JID 3987

To appear in: *The Journal of Investigative Dermatology*

Received Date: 14 February 2023

Accepted Date: 20 February 2023

Please cite this article as: Verkerk AJMH, Andrei D, Vermeer MCSC, Kramer D, Schouten M, Arp P, Verlouw JAM, Pas HH, Meijer HJ, van der Molen M, Oberdorf-Maass S, Nijenhuis M, Romero-Herrera PH, Hoes MF, Bremer J, Slotman JA, van den Akker PC, Diercks GFH, Giepmans BNG, Stoop H, Saris J, van den Ouweland AMW, Willemsen R, Hublin J-J, Dean MC, Hoogeboom AJM, Silljé HHW, Uitterlinden AG, van der Meer P, Bolling MC, Disruption of tuftelin 1, a desmosome associated protein, causes skin fragility, woolly hair and palmoplantar keratoderma, *The Journal of Investigative Dermatology* (2023), doi: https://doi.org/10.1016/j.jid.2023.02.044.

Disruption of tuftelin 1, a desmosome associated protein, causes skin fragility, woolly hair and palmoplantar keratoderma

Annemieke J.M.H. Verkerk[1]#, Daniela Andrei[2]#, Mathilde C.S.C. Vermeer[3], Duco Kramer[2], Marloes Schouten[3], Pascal Arp[1], Joost A.M. Verlouw[1], Hendri H. Pas[2], Hillegonda J. Meijer[2], Marije van der Molen[2], Silke Oberdorf-Maass[3], Miranda Nijenhuis[2], Pedro H. Romero-Herrera[3], Martijn F. Hoes[3], Jeroen Bremer[2], Johan A. Slotman[4], Peter C. van den Akker[5], Gilles F.H. Diercks[6], Ben N.G. Giepmans[7], Hans Stoop[8], Jasper Saris[9], Ans M.W. van den Ouweland[9], Rob Willemsen[9], Jean-Jacques Hublin[10,11], M. Christopher Dean[12,13], A. Jeannette M. Hoogeboom[9], Herman H.W. Silljé[3], André G. Uitterlinden[1], Peter van der Meer[3], Maria C. Bolling[2]

# These two authors contributed equally (shared first authors)

[1]*Erasmus MC, University Medical Center Rotterdam, Department of Internal Medicine, Rotterdam, The Netherlands.* [2]*University of Groningen, University Medical Centre Groningen, Department of Dermatology, Expertise Center for Blistering Diseases, Groningen, The Netherlands.* [3]*University of Groningen, University Medical Centre Groningen, Department of Cardiology, Groningen, The Netherlands.* [4]*Erasmus MC, University Medical Center Rotterdam, Optical Imaging Center, Rotterdam, The Netherlands.* [5]*University of Groningen, University Medical Centre Groningen, Department of Genetics, Expertise Center for Blistering Diseases, Groningen, The Netherlands.* [6]*University of Groningen, University Medical Centre Groningen, Department of Pathology, Groningen, The Netherlands.* [7]*University of Groningen, University Medical Centre Groningen, Department of Biomedical Sciences of Cells and Systems, Groningen, The Netherlands.* [8]*Erasmus MC, University Medical Center Rotterdam,*

Department of Pathology, Rotterdam, The Netherlands. [9]*Erasmus MC, University Medical Center Rotterdam, Department of Clinical Genetics, Rotterdam, The Netherlands.* [10]*Max Planck Institute for Evolutionary Anthropology, Department of Human Evolution, Leipzig, Germany.* [11]*Paléoanthropologie Collège de France, Paris, France.*[12]*Department of Earth Sciences, Natural History Museum, London, UK.* [13]*Department of Cell and Developmental Biology, University College London, London, UK.*

Corresponding author:

Annemieke J.M.H. Verkerk: j.verkerk@erasmusmc.nl

ABBREVIATIONS:

BMZ (basement membrane zone), DSC1-3 (desmocollin 1-3), DSG1-4 (desmoglein1-4), DSP (desmoplakin), EF (ejection fraction), EM (electron microscopy), ESV/EDV (end systolic/diastolic volumes), GFP= green fluorescent protein, IFs (intermediate filaments), JUP (plakoglobin), KDA (keratinocyte dissociation assay), KO (knock-out mouse), KRT5/6/14 (keratin 5/6/14), LV/RV (left/ right ventricle), MRI (magnetic resonance imaging), MYH6 alpha myosin heavy chain), MYH7 (beta myosin heavy chain), NMD (nonsense-mediated mRNA decay), NPPA (atrial natriuretic peptide), NPPB (brain natriuretic peptide), PKP1-3 (plakophilin 1-3), PPK (palmoplantar keratoderma), SNP (single nucleotide polymorphism), SV (stroke volume), TUFT1 (tuftelin 1), WES (whole exome sequencing), WH (woolly hair), WT (wild type mouse).

ABSTRACT

Desmosomes are dynamic complex protein structures involved in cellular adhesion. Disruption of these structures by loss of function variants in desmosomal genes lead to a variety of skin and heart related phenotypes. Here, we report tuftelin 1 as a desmosome-associated protein, implicated in epidermal integrity.

In two siblings with mild skin fragility, woolly hair and mild palmoplantar keratoderma, but without a cardiac phenotype, we identified a homozygous splice site variant in the *TUFT1* gene, leading to aberrant mRNA splicing and loss of tuftelin 1 protein. Patients' skin and keratinocytes showed acantholysis, perinuclear retraction of intermediate filaments, and reduced mechanical stress resistance. Immunolabeling and transfection studies showed that tuftelin 1 is positioned within the desmosome and its location dependent on the presence of the desmoplakin carboxy-terminal tail. A *Tuft1* knock-out mouse model mimicked the patients' phenotypes. Altogether, this study reveals tuftelin 1 as a desmosome-associated protein, whose absence causes skin fragility, woolly hair and palmoplantar keratoderma.

INTRODUCTION

The epidermis is the outermost skin layer, which is remarkably resistant to high levels of mechanical stress. An important complex to support strength and flexibility to the epidermal cell-cell contact is the desmosome, a dynamic structure with critical adhesive functions, whose components are regulated during tissue remodeling and differentiation(Nekrasova and Green 2013). This structure is a spot weld site that confers robust intercellular cohesion through the anchorage of intermediate filaments (IFs) to the plasma membrane. Since the discovery of the fundamental structure of desmosomes more than 60 years ago(Obland 1958), various studies contributed to discover their components, belonging to three major protein families: cadherins (desmogleins 1-4; desmocollins 1-3), armadillo proteins (plakoglobin, plakophilins 1-3), and plakins (desmoplakin, plectin)(Green and Simpson 2007a)(Lee and McGrath 2021). In skin, the desmosomes are connected to each other and with the nucleus by a network of circumferential and radial IFs composed of different keratins(Quinlan et al. 2017).

Disease-associated variants in genes encoding desmosomal proteins or their regulators can cause peeling, erosive or blistering skin disorders, as well as non-syndromic woolly hair (WH) or palmoplantar keratoderma (PPK)(Najor 2018; Vermeer et al. 2022). Desmosomes also have an important function in the heart, reflected by loss of function variants in desmoplakin (*DSP*)(McKoy et al. 2000; Norgett 2000), plakoglobin (*JUP*)(McKoy et al. 2000; Norgett 2000), and desmocollin 2 (DSC2)(Beffagna et al. 2007; Gehmlich et al. 2011), which can cause non-syndromic cardiomyopathy and cardiocutaneous syndromes(Vermeer et al. 2022). In recent years, significant progress has been made in the identification and characterization of different genes involved in skin fragility and related disorders, however, approximately 15% of the cases remain genetically unsolved(Has et al. 2020; Takeichi et al. 2015).

Here, we have identified and characterized the desmosome-associated protein, tuftelin 1 (TUFT1, encoded by the gene *TUFT1*), loss of which causes desmosomal dysfunction with skin

fragility, woolly hair and PPK in humans and mice. Previously TUFT1 was linked to processes such as enamel mineralization(Deutsch et al. 1991) chondrogenesis(Sliz et al. 2017) and tumorigenesis(Deutsch et al. 1991; Sliz et al. 2017; Zhou et al. 2016). Very recently, biallelic loss-of-function variants in *TUFT1* have been associated with a peeling skin phenotype with woolly hair in three pedigrees(Jackson et al. 2022). Here, we present an additional two siblings with a similar phenotype, and provide functional data, including from a *Tuft1* knockout mouse model, that designate TUFT1 as a desmosome-associated protein that plays a critical role in cell-cell adhesion and skin and hair morphogenesis.

RESULTS

Skin fragility, woolly hair and focal PPK observed in two Dutch siblings

Upon clinical investigation, two children, born to healthy parents from a small Dutch family of Caucasian ancestry, were diagnosed with skin fragility, woolly hair and focal PPK (**Figure 1**). Both affected children had light colored, tightly curled scalp hair, eyelashes (**Figure 1a, 1b, 1f**), eyebrows and body hairs. The skin fragility was mild with focal erosions resembling peeling of skin and occasionally vesicles/blisters upon everyday mechanical traumas (**Figure 1b-d, h**) and was more prevalent in summer than in winter. Mild focal PPK and extensive keratosis pilaris was seen (**Figure 1e, 1g**, **1i, 1j**). The teeth were all present and had a normal appearance, although both affected persons reportedly had a higher tendency to caries compared to the unaffected family members. Cardiological examination did not reveal any apparent abnormalities on electrocardiogram or ultrasound on different time points during clinical follow up (last time points at 17 and 19 years of age).

A homozygous splice variant in the *TUFT1* gene leads to alternative splicing with a frameshift and premature termination codon

Single Nucleotide Polymorphism (SNP) array analysis on DNA of the two patients identified several homozygous regions (**Supplementary Table 1a**), suggesting consanguinity of the parents. Variant filtering of Whole Exome Sequencing (WES) data of the two patients and their father, assuming recessive inheritance (**Figure 2a**, **Supplementary Table 1b**), combined with selection of variants residing in the identified homozygous areas, identified a homozygous splice acceptor site variant in intron 8, c.724-2A>G (chr1:151.547.385, build 37, NM_020127.2; ENST00000368849), of the *TUFT1* gene in the two affected children, whereas the father was a heterozygous carrier for this variant. Sanger sequencing validation confirmed these findings and in addition showed the mother to be a heterozygous carrier as well (**Figure 2b**). Splice site analysis programs (Alamut v.2.7.2) predicted skipping of exon 9 to be the most likely outcome and given the 100% evolutionary conserved sequence of the -2A splice acceptor site, this nucleotide change was expected to destroy the splice acceptor site of intron 8(Zhang 1998). This variant was not present in the gnomAD database (v2.1.1)(Lek et al. 2016) or any other public population variant frequency database. None of the known genes involved in skin fragility and cardiocutaneous syndromes, as mentioned in **Supplementary table 2**, were located in any of the identified homozygous regions, nor revealed any variants indicative to be disease-causing. RT-PCR was performed on lymphocyte mRNA from the patients and both parents and revealed alternative splicing leading to a frameshift and premature termination codon (**Figure 2c, 2d, Supplementary Figure 1a**). As aberrant splicing of exon 9 was predicted (Alamut v2.7.2), primers were designed on exon 5/6 and exon 11 to produce RT-PCR fragments. In a normal control this produced a 579 bp fragment as calculated. With the predicted skipping of exon 9, a 95 bp shorter fragment (484 bp) was expected and indeed observed in the affected children. However, also a larger fragment (602 bp) was present. With Sanger sequencing, this fragment was shown to contain 23 base pairs from intron 8 plus the complete

exon 9. Due to the loss of the original splice nucleotide, additionally, an alternative splice acceptor site (AG) in intron 8 was used (**Supplementary Figure 1a**), retaining 23 bases from intron 8, as well as exon 9 in this fragment. Based on signal intensities it was estimated that the alternative acceptor site was used in approximately 50% of the transcripts, retaining 23 bases from intron 8 and including exon 9, and in approximately 50% of the transcripts exon 9 was skipped. No normal cDNA product was observed. The heterozygous parents each showed the normal 579 bp cDNA fragment and the aberrant 484/602 bp fragments. In a healthy control only the 579 bp transcript with the normal exon 9 sequence was found **(Figure 2d)**. Hence, the identified splice site variant leads to a frameshift and premature stop codon for both aberrant cDNA products.

Nonsense mediated RNA decay leads to loss of TUFT1 protein

To determine the possible contribution of nonsense-mediated mRNA decay (NMD) of mutated mRNA, we investigated the relative expression levels of *TUFT1* mRNA in cultured skin fibroblast cells from one patient and two age matched controls. Cells were incubated with and without cycloheximide, a translation inhibitor that blocks mRNA NMD(Noensie and Dietz 2001; Schweingruber et al. 2013) (**Figure 2f**). A 3700x fold increase was observed in the patient *TUFT1* mRNA levels, in contrast with only a 25x and a 48x fold increase in the controls, indicating NMD mRNA degradation for the mutated *TUFT1* transcript in the patients. Western blot of patient's keratinocytes' extract with a TUFT1 C-terminal antibody showed absence of TUFT1 protein (**Figure 2e**). Quantitative PCR of *TUFT1* transcripts showed strong reduction in patient's keratinocytes and fibroblasts (**Supplementary Figure 2a and 2b**).

Patient skin shows strongly reduced TUFT1 expression and structural abnormalities

Haematoxylin and eosin (H&E) staining of perilesional skin biopsy sections from patient II1 showed mild acanthosis, spongiosis with marked intercellular widening with tendency to acantholysis and a sub-corneal split (**Figure 3a**). Immunofluorescent staining of TUFT1 on control human skin showed an epidermal cell membrane expression pattern and a strong reduction to near absence in patient's skin (**Figure 3b**). The basement membrane zone (BMZ) staining in control and patient skin was non-specific, as in *Tuft1* knockout mice the epidermal cell membrane staining of this antibody (antibody N3C3) disappeared, but the BMZ staining remained (**Supplementary figure 5b**). Additional stainings for BMZ and other desmosomal proteins and different keratins on patient II1 skin biopsies did not indicate any reduction or upregulation (**Supplementary Figure 3a**). Electron microscopy (EM) of patient II1's skin biopsy revealed keratin IF detachment at the inner dense plaque of the desmosomes and their retraction towards the nucleus in thick, dense clusters (**Figure 3c, lower panels**).

Patients' keratinocytes show structural abnormalities and weakened cell-cell contacts

Upon analyzing the morphology of the patients' cultured keratinocytes on H&E, keratinocytes from both patients (II1 and II2) showed significantly larger intercellular spaces, compared to healthy control keratinocytes (**Figure 4a, upper panels, Figure 4b**).

TUFT1 staining on control keratinocytes showed a cell-cell border staining, resembling desmosomes-like dotted patterns in control cells, while being completely absent in patient cells (**Figure 4a middle panels, Figure 4c**). In addition, DSP, a protein necessary to maintain desmosomal integrity(Vasioukhin et al. 2001), had a disturbed and more focal distribution along the cell borders in the patient cells (**Supplementary Figure 3b**). The IF KRT5 showed a strong retraction in the proximity of the nucleus in patients' cells (**Figure 4a, lower panels)**. The keratinocytes' total protein quantification of the desmosomal/ IF proteins by western blot analysis did not show any significant dysregulation. (**Supplementary Figure 3c**).

Assessment of the *in vitro* intercellular adhesiveness of keratinocytes through a keratinocyte dissociation assay (KDA), by subjecting detached keratinocyte monolayers to controlled mechanical stress via pipetting(Hartlieb et al. 2013; Simpson et al. 2010), showed extensive fragmentation of the patients' keratinocyte monolayer, compared to intact monolayers of control keratinocytes. Altogether, these data underpin that TUFT1 is involved in desmosomal cell-cell contact (**Figure 4d**).

TUFT1 localizes at keratinocyte cell-cell borders, co-localizes with desmosomal proteins and depends on DSP expression

Co-transfection of human keratinocytes (HaCaT) with a GFP labeled TUFT1 plasmid and either mCherry-DSG2 or mApple-KRT14, showed that TUFT1 co-localized at the plasma membrane with the desmosomal protein DSG2 which is mainly expressed in cultured keratinocytes (**Figure 5a, upper panels**), and with IF KRT14 at the membrane insertion site (**Figure 5a, lower panels**). To accurately localize TUFT1 within the desmosome we performed superresolution microscopy (direct stochastic optical reconstruction microscopy: dSTORM)(Xu et al. 2017). TUFT1 flanked both the transmembrane protein DSG3 and the anchoring protein DSP on the intracellular side, and consequently TUFT1 localized closest to the desmosomal intermediate filaments, at the inner dense plaque. Plaque to plaque distance measurements of DSP, as previously shown within a similar range as our current results(Stahley et al. 2016), are shown next to TUFT1 measurements, which show a slightly bigger median distance than DSP (**Figure 5b)**. TUFT1 also closely co-localized with DSC3 and the IFs KRT14 and KRT6 (**Supplementary Figure 4a**). Additionally, EM immunolabeling of TUFT1 on cultured primary keratinocytes, positioned TUFT1 on the cytoplasmic side of the desmosome, at the inner dense plaque, corroborating the dSTORM results (**Figure 5c**). TUFT1 protein

expression in culture conditions was dependent on calcium concentration (**Supplementary Figure 4b**), similar as is known for other desmosomal proteins(Watt et al. 1984).

Furthermore, we investigated whether TUFT1 protein expression within the desmosome was dependent on the desmosomal components, DSP (associated with severe skin fragility(Jonkman et al. 2005) and plakophilin 1 (PKP1), using available knockout/mutated primary keratinocytes lines(Jonkman et al. 2005). In keratinocytes from a patient with lethal acantholytic epidermolysis bullosa due to a compound heterozygous variant in *DSP* (*DSP*:c.6370delTT/c.6069C>T) causing a carboxyl-terminal truncation(Jonkman et al. 2005), TUFT1 failed to stain at the cell-cell border while plakoglobin still did. This suggests that TUFT1 association within the desmosome is DSP C-terminal dependent (**Figure 5d**). TUFT1 still localized at the cell-cell border in PKP1 deficient primary human keratinocytes (homozygous *PKP1*: c.1680+1G>A (NM_001005337.3) (**Supplementary Figure 4c**) indicating that TUFT1-DSP dependency is specific. However, this dependency is not mutual as DSP still localized at the cell membrane of TUFT1 mutated patients' cells, albeit in a different, more clustered-punctate pattern (**Supplementary Figure 3b**).

Tuft1 knock-out (KO) causes woolly hair and spontaneous skin erosions in mice

Tuft1 deficient mice presented with a woolly/wavy hair phenotype (**Figure 6a**)(Brown and Moore 2012) and groove-shaped hairs upon scanning EM analysis (**Supplementary Figure 5a**). Fourteen out of thirty-five homozygous KO mice developed spontaneous skin fragility over time due to grooming, scratching and/or fighting compared to none of the WT mice (**Figure 6c, d**). Heterozygous mice did not show any hair or skin abnormalities. The first skin erosion outbursts in KO mice seemed to start a cascade of itching reactions which worsened the phenotype over time. Measures such as isolating affected mice or nail cutting did not improve animal welfare, thus, affected mice were sacrificed due to humane endpoints. H&E staining of

the wounded skin showed a suprabasal split in the epidermis, with acantholysis and acanthosis (**Figure 6e, f**). TUFT1 immunofluorescence staining of the WT skin showed an epidermal staining (**Figure 6g**) and was completely negative in KO mice (**Figure 6h**). Immunofluorescent stainings of other desmosomal/hemidesmosomal proteins on mouse skin did not show significant differences **Supplementary Figure 5b**.

On ultrastructural levels, the spontaneous wounds showed blister fluid under a thick scab roof (**Figure 6j**) and abnormal keratinocytes with keratin bundle retraction in the proximity of the nucleus (**Figure 6k**). The desmosomes from the blister region, were "free-floating" in the extracellular space in the proximity of their adjacent cells, indicating their detachment from the IFs (**Figure 6l**).

Tuft1 KO mouse keratinocytes show abnormal differentiation and cytoplasmic DSP accumulation

KO mouse keratinocytes show a significant down-regulation of loricrin and involucrin, two late-stage differentiation markers(Tharakan et al. 2010) predominantly expressed in the upper suprabasal layers of the epidermis (**Figure 6m**). This suggests abnormalities within the differentiation processes as also indicated by the acanthosis observed in patient's skin and KO mouse skin. For DSP a significant up-regulation was observed in these cells (**Figure 6m**) with a predominant accumulation in the cytoplasm (Figure 6n). WB of other desmosomal and IF proteins were not significantly affected in TUFT1 deficient mouse keratinocytes (**Supplementary Figure 5c**) and the desmosomes morphometrics were not significantly different (**Supplementary Figure 5d**). KRT5 staining showed a slight nuclear retraction, leaving wider gaps in between cells (**Figure 6n**).

TUFT1 KO leads to differential expression of genes involved in epidermal homeostatis

RNAseq analysis on WT and healthy parts of KO skin resulted in 21 significantly differentially expressed genes (FDR<0.05) (**Supplementary Table 9**). Thirteen were downregulated, and 8 upregulated. The downregulated genes, *Lep*(Collin et al. 2017) *Serpine1*(Subramaniyam et al. 2010), and *CD36*(Pohl et al. 2005)are involved in lipid rafts remodeling, a process previously shown to be involved in desmosomes assembly and intercellular adhesion(Resnik et al. 2011). Two upregulated genes, *s100a4* and *Krt6a* were previously shown to be involved in hyperkeratotic and inflammatory diseases such as psoriasis(Zibert et al. 2010) and pachyonychia congenita (Forrest et al. 2016). Additionally, a publicly available GEO dataset showed 5 genes in a human epidermal injury model, that show the same trendline of expression (upregulation of downregulation) as our KO *Tuft1* murine model (**Supplementary figure 5e**).

TUFT1 localizes in the heart at the intercalated discs, but no significant cardiac abnormalities were present in *Tuft1* KO mice

Hearts of KO mice at age 12 months, were not morphometrically different from WT (**Supplementary Figure 6a**). In WT heart tissue, TUFT1 specifically localized at the intercalated discs, similar to the desmosomal proteins DSP and DSC2 (**Supplementary Figure 6b**) and was absent in KO. No significant differences between WT and KO mice were found on magnetic resonance imaging (MRI) analysis, showing normal end systolic/diastolic volumes (ESV, EDV), ejection fraction (EF), stroke volume (SV) and systolic/diastolic myomass of the left and right ventricles (LV, RV) (**Supplementary Figure 6c, 6d**). Also, mRNA expression of cardiac injury markers(Eijgenraam et al. 2020) atrial natriuretic peptide (*Nppa*), brain natriuretic peptide (*Nppb*), alpha myosin heavy chain (*Myh6*) and beta myosin heavy chain (*Myh7*) were not significantly different in the LV and RV of KO mice (**Supplementary Figure 6e**). In hearts of WT mice, *Tuft1* mRNA expression levels were 2-4 times lower than in skin (**Supplementary Figure 6f**).

Patients' molar does not show any abnormalities

As TUFT1 was previously suggested to play a role during development and mineralization of enamel(Deutsch et al. 1991), we investigated the lower right deciduous second molar tooth of one of the patients. Micro-CT scan did not reveal any peculiar features regarding metrics or morphology. While there was some localized surface enamel demineralization and pitting hypoplasia, there was no evidence of any generalized structural or maturational enamel defects (**Supplementary Figure 7 a,b,f)**. Investigation of 4 histological ground sections showed a neonatal line (NNL) in the enamel that was normally positioned and of normal thickness (**Supplementary Figure 7 c-i**).

DISCUSSION

Desmosomes are essential cell-cell connecting structures in different stress-bearing tissues, in particular in skin and heart(Green and Simpson 2007b). Here, we identified TUFT1 as a desmosome associated component, localizing at the DSP-IF interface of the inner dense plaque. Similar to other desmosomal proteins, TUFT1 expression in cultured keratinocytes is calcium-dependent. In addition, its localization is dependent on the DSP C-terminal domain. In a previous yeast two-hybrid study(Paine et al. 1998), TUFT1 was suggested to interact with keratin-5/6, two epidermal expressed proteins that connect to the desmosome. More recently, TUFT1 was identified among several proteins possibly associated with the desmosome in a mass spectrometry analysis using DSP C-terminal and N-terminal constructs as baits(Badu-Nkansah and Lechler 2019).

Using homozygosity mapping and whole exome sequencing, a disease-causing splice variant in the *TUFT1* gene, leading to aberrant splicing and a frameshift with loss of protein, was identified in two affected children with skin fragility, woolly hair and palmoplantar

keratoderma. Very recently, bi-allelic loss-of-function *TUFT1* variants were identified in nine other patients with woolly hair and skin fragility(Jackson et al. 2022). Our study demonstrates that loss of TUFT1 leads to abnormalities in desmosomal morphology, weakened cell-cell contacts, reduced stress resilience of the cell-cell connection and differentiation disturbances (Wan et al. 2004). In addition our functional data show that loss of TUFT1 causes desmosome-IF connection defects in patient-derived keratinocytes and directly places TUFT1 within the inner dense plaque of the desmosome. Moreover, we show that *Tuft1* knockout in mice reveals a strikingly similar phenotype as in humans and that the cardiac tissue seems to be spared despite expression of TUFT1 therein.

In contrast to mouse knock-outs for *Jup*(Bierkamp et al. 1996), *Dsp*(Vasioukhin et al. 2001), *Pkp1*(Katrin Rietscher 2018) and *Dsg1*(Kugelmann et al. 2019), *Tuft1* knock-outs are compatible with life. All knock-out mice showed abnormal fur with a wavy appearance mimicking the woolly hair observed in the patients. In addition, 40% of KO mice developed spontaneous erosions, with disturbed keratinocyte cell-cell contacts, and impaired IF insertion to the desmosome. The fact that not all mice developed a skin fragility phenotype may depend on the mildness of the skin fragility phenotype, also described by Jackson et al., as a phenotypic characteristic in most of the affected patients but not present in all.

Despite TUFT1 expression at the intercalated discs of myocardium, no apparent cardiac phenotype was observed in the *TUFT1* negative patients (at the age of 17 and 19), nor in the *Tuft1* knockout mice until the age of 12 months. However, cardiac involvement cannot be completely ruled out at this point as no patients older than 23 years have ever been cardiologically evaluated(Jackson et al. 2022). Additional studies are necessary to get more insight whether TUFT1 plays a role in cardiac function.

Previously, TUFT1 was identified as being involved in the process of enamel mineralization(Deutsch et al. 1991). However, histological analysis of a patient's deciduous

molar did not show any abnormalities in enamel or dentine formation. TUFT1 has also been reported to be involved in processes like chondrogenesis(Sliz et al. 2017) and tumorigenesis(Dou et al. 2019; Liu et al. 2019; Liu et al. 2018; Zhou et al. 2016)and additionally was shown to have a more widespread distribution with likely tissue dependent functions(Leiser et al. 2007). Whether TUFT1 is a structural or a regulatory protein for the desmosome is not clear at the moment, but it does not seem to be essential for desmosome formation or embryonic development of tissues like skin or heart. Nevertheless, lack of TUFT1 clearly affects desmosomal function and cell-cell connection. Pathogenic variants in other desmosomal genes, like i.e. *DSP*, may cause a variety of phenotypes, involving either skin or heart, or both. Whether different pathogenic variants in *TUFT1* may result in a variety of phenotypic effects, cannot be determined at the moment. Nonetheless, our data implicate the *TUFT1* gene and its encoding protein in the maintenance of skin integrity and in human monogenetic disease.

In summary, this study identifies TUFT1 as a protein involved in human skin fragility and hair disorders and defines it as a desmosome-associated protein.

MATERIALS AND METHODS

Patients

In the diagnostic setting clinical photographs, hair samples, skin biopsies and blood were taken. Written informed consent (University Medical Centre Groningen) was obtained from the parents to use the left-over clinical material for research purposes and publication. Written informed consent (Erasmus Medical Centre) was obtained from the parents for publication of the images.

Mice

Wildtype and homozygous *TUFT1* knock-out mice (Tuft1$^{tm1a(KOMP)Wtsi}$) in a C57BL/6NTac background were produced by the International Mouse Phenotyping Consortium (IMPC, Wellcome Trust Sanger Institute, https://www.mousephenotype.org/data/genes/MGI:109572. The study was approved by the local Animal Ethics committee (The Netherlands) license number: AVD199105-01-002. ARRIVE guidelines(Percie du Sert et al. 2020) were used for reporting this study. Our study comprised both a 3-months and a 12-months old group.

Data Availability Statement

Additional materials and methods are added as a supplement. RNA sequencing data can be accessed at the GEO database with: GSE237986. Nanotomy images can be accessed under www.nanotomy.org

CONFLICT OF INTEREST

PvdM received consultancy fees and/or grants from Novartis, Pharmacosmos, Vifor Pharma, Astra Zeneca, Pfizer, Abbott, Pharma Nord, Novo Nordisk, BridgeBio and Ionis, all paid to the institute. The remaining authors have declared no conflict of interest.

ACKNOWLEDGMENTS

We thank the family, and especially the children, for their continuous cooperation, their endless patience, perseverance and trust. We acknowledge the late Prof.dr. A.P. Oranje for his many years of dedicated supervision of the family. We thank Joke Polak and Nicole van Koetsveld for fibroblast cell culture, Lida Prins-Bakker, Lies-Anne Severijnen for experimental and technical support, the late Michael Davidson and Michelle Baird from the USA for cloning fluorescent constructs, and Suzanne Pasmans, Senada Koljenović, Max Kros and Alice Brooks for fruitful discussions. We thank Inge Bruins for her experimental contributions during her

thesis. We thank Stichting Vlinderkind for the financial support to perform the studies.

Part of the work has been performed in the UMCG Microscopy and Imaging Center (UMIC), sponsored by ZonMW grant 91111.006 and the Netherlands Electron Microscopy Infrastructure (NEMI; NWO 184.034.014)

Author contributions

Conceptualization - AJMHV, DA, PvdM, MCB

Methodology - AJMHV, DA, DK, MHH, JB, PCvdA, HHWS, PvdM, MCB

Software -

Validation - PA, MHH, AMWvdO, PvdM, MCB

Formal Analysis - DA, AJMHV, MCSCV, DK, PA, JAMV, MCB

Investigation - DA, AJMHV, MCSCV, DK, MS, PA, HJM, MvdM, SO-M, AMN, PHR-H, JAS, GFHD, HS, JJS, MCD, AJMH

Resources - AJMHV, JB, JAS, BNGG, JJH, AJMH, HHWS, AGU, PvdM, MCB

Data Curation- DA, JAMV

Writing – Original Draft Preparation - AJMHV, DA, MCD, MCB

Writing – Review and Editing - All Authors

Visualization – DA, AJMHV

Supervision - AJMHV, HHP, JB, PvdM, MCB

Project Administration - AJMHV, PvdM, MCB

Funding Acquisition - AGU, PvdM, MCB

REFERENCES

Badu-Nkansah K, Lechler T. Proteomic analysis of the desmosome identifies novel components required for skin integrity.pdf. 2019;

Beffagna G, de Bortoli M, Nava A, Salamon M, Lorenzon A, Zaccolo M, et al. Missense mutations in Desmocollin-2 N-terminus, associated with arrhythmogenic right ventricular cardiomyopathy, affect intracellular localization of desmocollin-2 in vitro. BMC Med Genet. 2007;8(1):65

Bierkamp C, Mclaughlin KJ, Schwarz H, Huber O, Kemler R. Embryonic Heart and Skin Defects in Mice Lacking Plakoglobin. Dev Biol. 1996;180(2):780–5 Available from: https://linkinghub.elsevier.com/retrieve/pii/S0012160696903462

Brown SDM, Moore MW. The International Mouse Phenotyping Consortium: past and future perspectives on mouse phenotyping. Mammalian Genome. 2012;23(9–10):632–40

Collin A, Noacco A, Talvas J, Caldefie-Chézet F, Vasson M-P, Farges M-C. Enhancement of Lytic Activity by Leptin Is Independent From Lipid Rafts in Murine Primary Splenocytes. J Cell Physiol. 2017;232(1):101–9

Deutsch D, Palmon A, Fisher LW, Kolodny N, Termine JD, Young MF. Sequencing of bovine enamelin ("tuftelin") a novel acidic enamel protein. J Biol Chem. 1991;266(24):16021–8 Available from: http://www.ncbi.nlm.nih.gov/pubmed/1874744

Dou C, Zhou Z, Xu Q, Liu Z, Zeng Y, Wang Y, et al. Hypoxia-induced TUFT1 promotes the growth and metastasis of hepatocellular carcinoma by activating the Ca2+/PI3K/AKT pathway. Oncogene. 2019;38(8):1239–55

Eijgenraam TR, Boukens BJ, Boogerd CJ, Schouten EM, van de Kolk CWA, Stege NM, et al. The phospholamban p.(Arg14del) pathogenic variant leads to cardiomyopathy with heart failure and is unresponsive to standard heart failure therapy. Sci Rep. 2020;10(1):9819

Forrest CE, Casey G, Mordaunt DA, Thompson EM, Gordon L. Pachyonychia Congenita: A Spectrum of KRT6a Mutations in Australian Patients. Pediatr Dermatol. 2016;33(3):337–42

Gehmlich K, Syrris P, Peskett E, Evans A, Ehler E, Asimaki A, et al. Mechanistic insights into arrhythmogenic right ventricular cardiomyopathy caused by desmocollin-2 mutations. Cardiovasc Res. 2011;90(1):77–87

Green KJ, Simpson CL. Desmosomes: New Perspectives on a Classic. Journal of Investigative Dermatology. 2007a;127(11):2499–515 Available from: https://linkinghub.elsevier.com/retrieve/pii/S0022202X1533164X

Green KJ, Simpson CL. Desmosomes: New Perspectives on a Classic. Journal of Investigative Dermatology. 2007b;127(11):2499–515 Available from: https://linkinghub.elsevier.com/retrieve/pii/S0022202X1533164X

Hartlieb E, Kempf B, Partilla M, Vigh B, Spindler V, Waschke J. Desmoglein 2 Is Less Important than Desmoglein 3 for Keratinocyte Cohesion. Gottardi C, editor. PLoS One. 2013;8(1):e53739 Available from: https://dx.plos.org/10.1371/journal.pone.0053739

Has C, Bauer JW, Bodemer C, Bolling MC, Bruckner-Tuderman L, Diem A, et al. Consensus reclassification of inherited epidermolysis bullosa and other disorders with skin fragility. British

Journal of Dermatology. 2020;183(4):614–27 Available from: https://onlinelibrary.wiley.com/doi/10.1111/bjd.18921

Jackson A, Celia Moss, Kate E Chandler, Pablo Lopez Balboa, Maria L Bageta, Gabriela Petrof, et al. Biallelic TUFT1 variants cause woolly hair, superficial skin fragility and desmosomal defects. British Journal of Dermatology. 2022;(ljac026)

Jonkman MF, Pasmooij AMG, Pasmans SGMA, van den Berg MP, ter Horst HJ, Timmer A, et al. Loss of Desmoplakin Tail Causes Lethal Acantholytic Epidermolysis Bullosa*. The American Journal of Human Genetics. 2005;77(4):653–60 Available from: https://linkinghub.elsevier.com/retrieve/pii/S0002929707610131

Katrin Rietscher. Regulation of PKP1´s function in intercellular adhesion, proliferation and barrier formation. Martin-Luther-Universität, Halle-Wittenberg. Halle-Wittenberg; 2018;98–103 Available from: https://opendata.uni-halle.de//handle/1981185920/9007

Kugelmann D, Radeva MY, Spindler V, Waschke J. Desmoglein 1 Deficiency Causes Lethal Skin Blistering. Journal of Investigative Dermatology. 2019;139(7):1596-1599.e2

Lee JYW, McGrath JA. Mutations in genes encoding desmosomal proteins: spectrum of cutaneous and extracutaneous abnormalities*. British Journal of Dermatology. 2021;184(4):596–605

Leiser Y, Blumenfeld A, Haze A, Dafni L, Taylor AL, Rosenfeld E, et al. Localization, quantification, and characterization of tuftelin in soft tissues. The Anatomical Record: Advances in Integrative Anatomy and Evolutionary Biology. 2007;290(5):449–54 Available from: https://onlinelibrary.wiley.com/doi/10.1002/ar.20512

Lek M, Karczewski KJ, Minikel E v., Samocha KE, Banks E, Fennell T, et al. Analysis of protein-coding genetic variation in 60,706 humans. Nature. 2016;536(7616):285–91 Available from: http://www.nature.com/articles/nature19057

Liu W, Chen G, Sun L, Zhang Y, Han J, Dai Y, et al. TUFT1 Promotes Triple Negative Breast Cancer Metastasis, Stemness, and Chemoresistance by Up-Regulating the Rac1/β-Catenin Pathway. Front Oncol. 2019;9

Liu H, Zhu J, Mao Z, Zhang G, Hu X, Chen F. Tuft1 promotes thyroid carcinoma cell invasion and proliferation and suppresses apoptosis through the Akt-mTOR/GSK3β signaling pathway. Am J Transl Res. 2018;10(12):4376–84 Available from: http://www.ncbi.nlm.nih.gov/pubmed/30662679

McKoy G, Protonotarios N, Crosby A, Tsatsopoulou A, Anastasakis A, Coonar A, et al. Identification of a deletion in plakoglobin in arrhythmogenic right ventricular cardiomyopathy with palmoplantar keratoderma and woolly hair (Naxos disease). The Lancet. 2000;355(9221):2119–24

Najor NA. Desmosomes in Human Disease. Annual Review of Pathology: Mechanisms of Disease. 2018;13(1):51–70

Nekrasova O, Green KJ. Desmosome assembly and dynamics. Trends Cell Biol. Elsevier Ltd; 2013;23(11):537–46

Noensie EN, Dietz HC. A strategy for disease gene identification through nonsense-mediated mRNA decay inhibition. Nat Biotechnol. 2001;19(5):434–9

Norgett EE. Recessive mutation in desmoplakin disrupts desmoplakin-intermediate filament interactions and causes dilated cardiomyopathy, woolly hair and keratoderma. Hum Mol Genet. 2000;9(18):2761–6

Obland GF. The Fine Structure of the Interrelationship of Cells in the Human Epidermis. J Biophys Biochem Cytolv. 1958;4(5):529–38 Available from: https://www.ncbi.nlm.nih.gov/pmc/articles/PMC2224536/

Paine CT, Paine ML, Snead ML. Identification of Tuftelin-and Amelogenin-Interacting Proteins Using the Yeast Two-Hybrid System. Connect Tissue Res. 1998;38(1–4):257–67 Available from: http://www.tandfonline.com/doi/full/10.3109/03008209809017046

Percie du Sert N, Hurst V, Ahluwalia A, Alam S, Avey MT, Baker M, et al. The ARRIVE guidelines 2.0: Updated guidelines for reporting animal research. PLoS Biol. 2020;18(7):e3000410

Pohl J, Ring A, Korkmaz Ü, Ehehalt R, Stremmel W. FAT/CD36-mediated Long-Chain Fatty Acid Uptake in Adipocytes Requires Plasma Membrane Rafts. Mol Biol Cell. 2005;16(1):24–31

Quinlan RA, Schwarz N, Windoffer R, Richardson C, Hawkins T, Broussard JA, et al. A rim-and-spoke hypothesis to explain the biomechanical roles for cytoplasmic intermediate filament networks. J Cell Sci. 2017;130(20):3437–45

Resnik N, Sepčić K, Plemenitaš A, Windoffer R, Leube R, Veranič P. Desmosome Assembly and Cell-Cell Adhesion Are Membrane Raft-dependent Processes. Journal of Biological Chemistry. 2011;286(2):1499–507

Schweingruber C, Rufener SC, Zünd D, Yamashita A, Mühlemann O. Nonsense-mediated mRNA decay — Mechanisms of substrate mRNA recognition and degradation in mammalian cells. Biochimica et Biophysica Acta (BBA) - Gene Regulatory Mechanisms. 2013;1829(6–7):612–23

Simpson CL, Kojima S, Cooper-Whitehair V, Getsios S, Green KJ. Plakoglobin Rescues Adhesive Defects Induced by Ectodomain Truncation of the Desmosomal Cadherin Desmoglein 1. Am J Pathol. 2010;177(6):2921–37 Available from: https://linkinghub.elsevier.com/retrieve/pii/S0002944010629197

Sliz E, Taipale M, Welling M, Skarp S, Alaraudanjoki V, Ignatius J, et al. TUFT1, a novel candidate gene for metatarsophalangeal osteoarthritis, plays a role in chondrogenesis on a calcium-related pathway. PLoS One. 2017;12(4):e0175474 Available from: http://www.ncbi.nlm.nih.gov/pubmed/28410428

Stahley SN, Bartle EI, Atkinson CE, Kowalczyk AP, Mattheyses AL. Molecular organization of the desmosome as revealed by direct stochastic optical reconstruction microscopy. J Cell Sci. 2016;

Subramaniyam D, Zhou H, Liang M, Welte T, Mahadeva R, Janciauskiene S. Cholesterol rich lipid raft microdomains are gateway for acute phase protein, SERPINA1. Int J Biochem Cell Biol. 2010;42(9):1562–70

Takeichi T, Liu L, Fong K, Ozoemena L, McMillan JR, Salam A, et al. Whole-exome sequencing improves mutation detection in a diagnostic epidermolysis bullosa laboratory. British Journal of Dermatology. 2015;172(1):94–100

Tharakan S, Pontiggia L, Biedermann T, Böttcher-Haberzeth S, Schiestl C, Reichmann E, et al. Transglutaminases, involucrin, and loricrin as markers of epidermal differentiation in skin substitutes derived from human sweat gland cells. Pediatr Surg Int. 2010;26(1):71–7 Available from: http://link.springer.com/10.1007/s00383-009-2517-5

Vasioukhin V, Bowers E, Bauer C, Degenstein L, Fuchs E. Desmoplakin is essential in epidermal sheet formation. Nat Cell Biol. 2001;3(12):1076–85 Available from: http://www.nature.com/articles/ncb1201-1076

Vermeer MCSC, Andrei D, Marsili L, van Tintelen JP, Silljé HHW, van den Berg MP, et al. Towards a Better Understanding of Genotype–Phenotype Correlations and Therapeutic Targets for Cardiocutaneous Genes: The Importance of Functional Studies above Prediction. Int J Mol Sci. 2022;23(18):10765

Watt FM, Mattey DL, Garrod DR. Calcium-induced reorganization of desmosomal components in cultured human keratinocytes. Journal of Cell Biology. 1984;99(6):2211–5

Xu J, Ma H, Liu Y. Stochastic Optical Reconstruction Microscopy (STORM). Curr Protoc Cytom. 2017;81(1) Available from: https://onlinelibrary.wiley.com/doi/10.1002/cpcy.23

Zhang M. Statistical features of human exons and their flanking regions. Hum Mol Genet. 1998;7(5):919–32 Available from: https://academic.oup.com/hmg/article-lookup/doi/10.1093/hmg/7.5.919

Zhou B, Zhan H, Tin L, Liu S, Xu J, Dong Y, et al. TUFT1 regulates metastasis of pancreatic cancer through HIF1-Snail pathway induced epithelial-mesenchymal transition. Cancer Lett. 2016;382(1):11–20 Available from: http://www.ncbi.nlm.nih.gov/pubmed/27566398

Zibert JR, Skov L, Thyssen JP, Jacobsen GK, Grigorian M. Significance of the S100A4 Protein in Psoriasis. Journal of Investigative Dermatology. 2010;130(1):150–60

FIGURE LEGENDS

Figure 1. Clinical phenotype of the two affected children, male (a-e) and female (f-j).

Images of: **(a)** the boy's woolly hair, including some bald spots at the age of 15, **(b)** curly eyelashes (asterisk) and mild erosions induced by wearing glasses (arrow), **(c, d)** mild skin fragility showing superficial erosions without severe blistering (arrow) **(d)** zoom-in of (c) and **(e)** palmar hyperkeratosis. Images of: **(f)** the girl's woolly hair, **(g)** hyperkeratosis on the soles of the feet, **(h)** mild skin erosions and a vesicle upon skin rubbing (arrow) and **(i)** keratosis pilaris, **(j)** microscopic image of (i) revealing the small hyperkeratotic plugs (arrow). Written informed consent was obtained from the parents for publication of the images.

Figure 2. Genetic analysis of the patients.

(a) Pedigree of the family. Filled symbols represent affected individuals and empty symbols represent healthy family members. Double line represents consanguinity of the parents. **(b)** DNA Sanger sequence validation showing the *TUFT1* splice mutation in intron 8 (c.724-2A>G). The normal sequence from intron 8 to exon 9 is acccagGAGCAT, with the last six bases of intron 8 indicated in lowercase letters and the first six bases of exon 9 in capital letters. The position of the mutation a>g is underscored. Homozygous mutation as seen in probands II1 and II2 (top panel) and heterozygous mutation in carrier parents I1, I2 (lower panel) are indicated by an arrowhead. **(c)** Electrophoretic analysis (labchip) shows RT-PCR products on lymphocyte RNA of patients II1 and II2, heterozygous carrier parents I1 and I2, and control (C). n=negative control without DNA. M=HT DNA HiSens ladder (Perkin Elmer) **(d)** Schematic view of *TUFT1* cDNA products identified in the family members after sequencing of the different RT-PCR products. Exon numbers are indicated. **(e)** Keratinocytes protein extracts tested by western blot. Patients (II1 and II2) protein quantification by western blot shows a complete absence of TUFT1 protein. C1, C2 and C3 are different donor controls. Antibodies are listed in supplementary table 5. **(f)** Effect of nonsense mediated mRNA decay inhibition (NMDi) on relative *TUFT1* mRNA expression levels in control and patient fibroblasts. After NMDi treatment, expression levels of mutated *TUFT1* transcripts in the patient increased 3700x fold as compared to *TUFT1* transcript levels in controls with 26x and 48x fold increase; Average Ct values: C1= 29.8, C1+NMDi= 24.2, C2= 27.9, C2+NMDi= 23.2, II1= 36.2, II1+NMDi= 23.9. Error bar=standard error mean (SEM), paired t test ***p<0,0005.

Figure 3. Patients' skin analysis.

(a) Patient II1 skin biopsy analysis (haematoxylin and eosin (H&E)) staining shows mild acanthosis and a sub-corneal split in the epidermis (upper arrow) with widened spaces between keratinocytes and mild acantholysis (lower arrow), compared to control. Scale bar 50 µm. **(b)**

Immunofluorescence microscopy of tuftelin 1 staining shows marked reduction at the epidermal cell surface in patient II1 skin compared to control. Note the non-specific basement membrane zone staining in the Ctrl and II1 (asterisk). Scale bar 50µm. Antibodies are listed in supplementary table 5. **(c)** Ultrastructural (EM) analysis of the skin shows perinuclear aggregation of intermediate filaments in patient II1 (lower panel, second image) with keratin intermediate filament disruption from the desmosome (lower panel, third image, red arrows). The patient desmosome structures appear normal, with an inner-dense plaque and outer dense plaque, (lower panel, fourth image). Boxes indicate regions of magnification. Scale bar 10 µm for the left images, 1 µm for second and third zoom-images and 500 nm for the fourth images.

Figure 4. *In vitro* primary keratinocytes characterization.

(a) Upper panels: H&E of cultured patient keratinocytes shows larger intercellular spaces compared to control cells. Scale bar 50µm. Middle panels: Tuftelin 1 immunofluorescence staining of keratinocytes (green) shows a cell-cell border staining in control cells (arrows), while this is absent in the patients. Lower panels: Keratin 5 staining (green) shows a perinuclear retraction of the intermediate filaments. Nuclear staining with DAPI (blue). Scale bar 50 µm. Antibodies are listed in supplementary table 5. **(b)** Quantification of the extracellular space shows that the area is significantly larger in both patients (ctrl represents 5 H&E images, II1 represents 3 and II2 4 H&E images) error bar SEM, unpaired t test **$p<0.005$; *$p<0.05$. **(c)** TUFT1 immunofluorescent intensity is quantified at the membrane; Mann-Whitney test *$p<0.05$. **(d)** Keratinocyte dissociation assay (KDA) shows extensive disruption of the patients' II1 and II2 keratinocytes monolayers in comparison with controls'.

Figure 5. Tuftelin 1 localization.

(a) HaCaT cells co-transfected with tuftelin 1-GFP and desmoglein 2-mCherry/ keratin 14-mApple shows co-localization of tuftelin 1 with the desmosomal proteins desmoglein 2 (DSG2) at the plasma membrane (upper panels), and keratin 14 (KRT14) intermediate filaments at the membrane insertion site (lower panels). Scalebar 50 µm. **(b)** Immunofluorescence staining with antibodies against TUFT1 (red), desmoglein 3 (DSG3) (green) and the desmoplakin c-terminal (DSP) (green) on primary human control keratinocytes analyzed via direct stochastic optical reconstruction microscopy (dSTORM) imaging shows that TUFT1 flanks both DSG3 and DSP, and localizes closest to DSP. Scale bar 1µm. Antibodies are listed in supplementary table 6. Plaque to plaque distance measurement in nanometers are shown in the box (25-75% box) and whiskers plots (10-90% whiskers) **(c)** TUFT1 immunolabeling on cultured control primary keratinocytes visualized by EM as gold nanoparticles (the white box indicates the magnified area on the right) shows localization of tuftelin 1 within the desmosome on the intracellular side. Black arrow= outer dense plaque; red arrow=inner dense plaque. Scale bar 1 µm. Antibodies are listed in supplementary table 7. **(d)** Cultured C-terminal truncated DSP (compound heterozygous *DSP* mutation: c.6370delTT/c.6069C>T) primary keratinocytes fail to show a membrane tuftelin 1 staining as is seen in the control (upper panel). The *DSP* mutated keratinocytes show remnants of desmosomes with plakoglobin (JUP) staining (lower panel). Magnified areas indicated with boxes are shown on the right) Scale bar 50µm. Antibodies are listed in supplementary table 5.

Figure 6. Mouse *Tuft1* knock-out (KO) characterization.

(**a**) Woolly hair of homozygous *Tuft1* KO mice and (**b**) straight hair of WT mice**. (c, d)** Wounds and erosions in KO mice. **(e)** Acanthosis and suprabasal epidermal split in lesional skin of KO mice (arrows) **(f)** compared to the epidermis of the WT mice. **(g)** Tuftelin 1 immunofluorescence staining shows an epidermal pattern in WT skin (green) (**h**) compared to

the KO skin which is completely negative**.** EM of: **(i)** WT skin, **(j)** spontaneous blistered KO skin with blister fluid depicted in pink, **(k)** with bundles of keratin filaments in the proximity of the nucleus (arrow), and magnification in **(l)** of intact but "free-floating" desmosomes (arrows) without keratin attachment in proximity of the blister fluid. BM=basement membrane; F=blister fluid; R=wound roof, scale bar i, j- 10 µm, k- 1 µm, l- 500 nm. **(m)** Keratinocytes cultured from 3-month old WT (n=4) and KO mice (n=6) analysed by western blot for the indicated proteins: TUFT1, DSP, loricrin (LOR) and involucrin (IVL), indicating a downregulation of LOR and IVL and an upregulation of desmoplakin in the KO mice. Error bar SEM, unpaired t test, **p<0.005; ***p<0.0005. **(n)** Immunofluorescence staining for TUFT1, DSP and KRT5 shows an upregulation and accumulation of DSP predominantly in the cytoplasm of the KO cells and wider intercellular spaces for KRT5 stained KO keratinocytes. Scale bar 50 µm. Antibodies are listed in supplementary table 5.

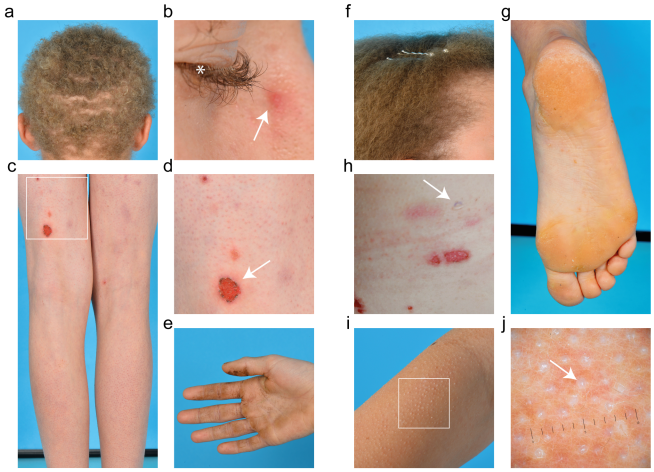

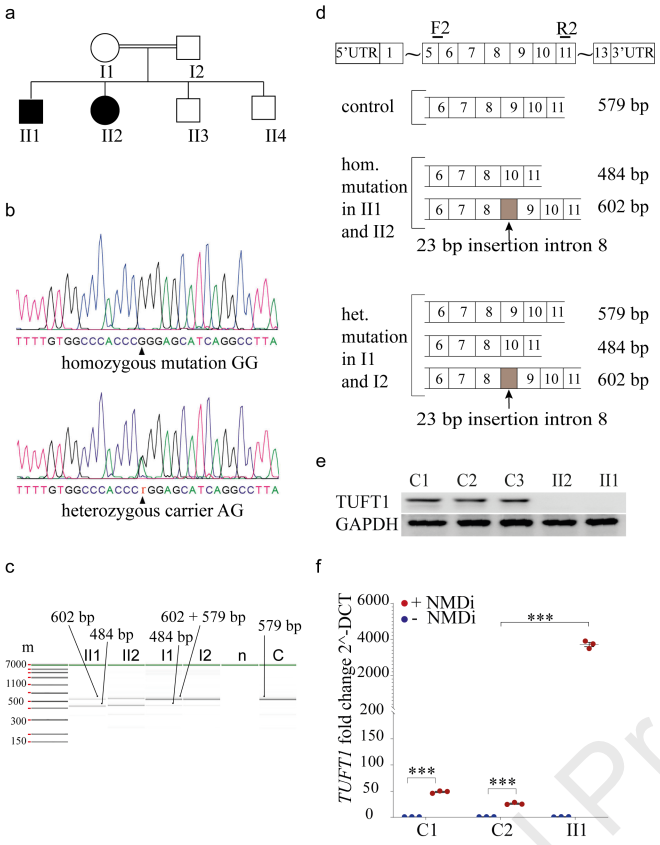

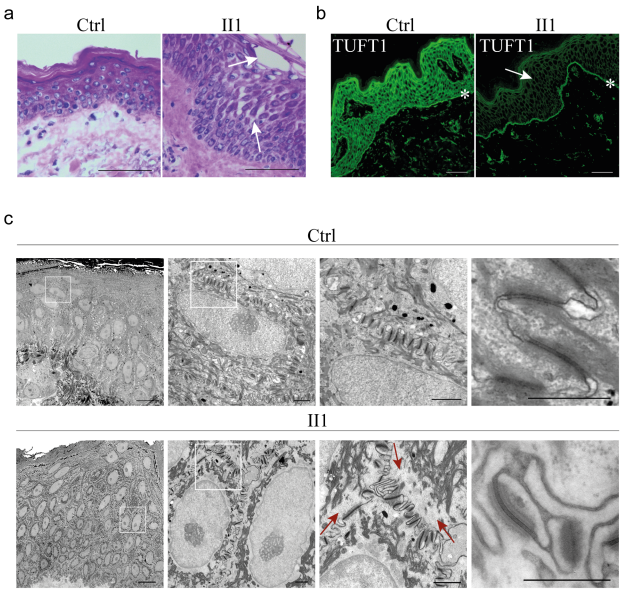

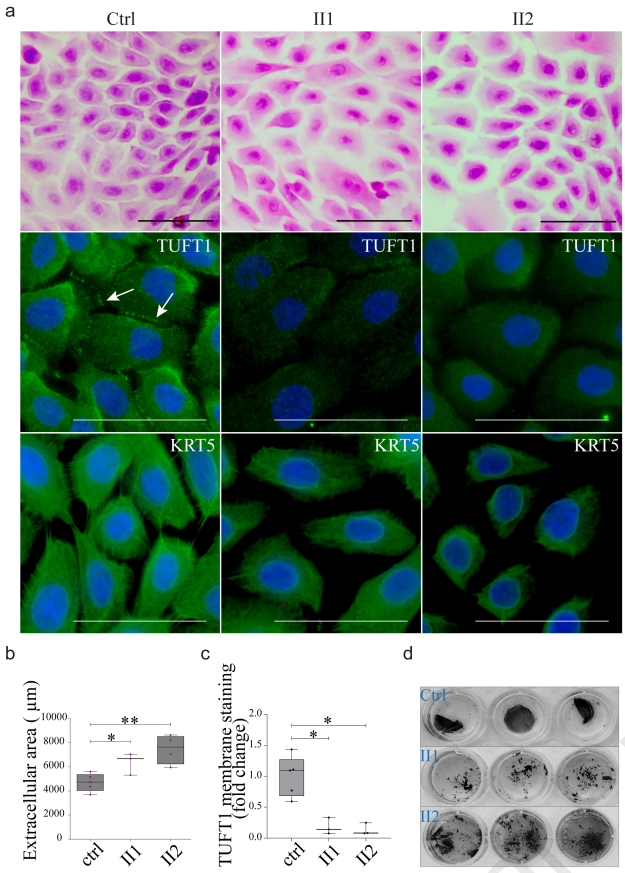

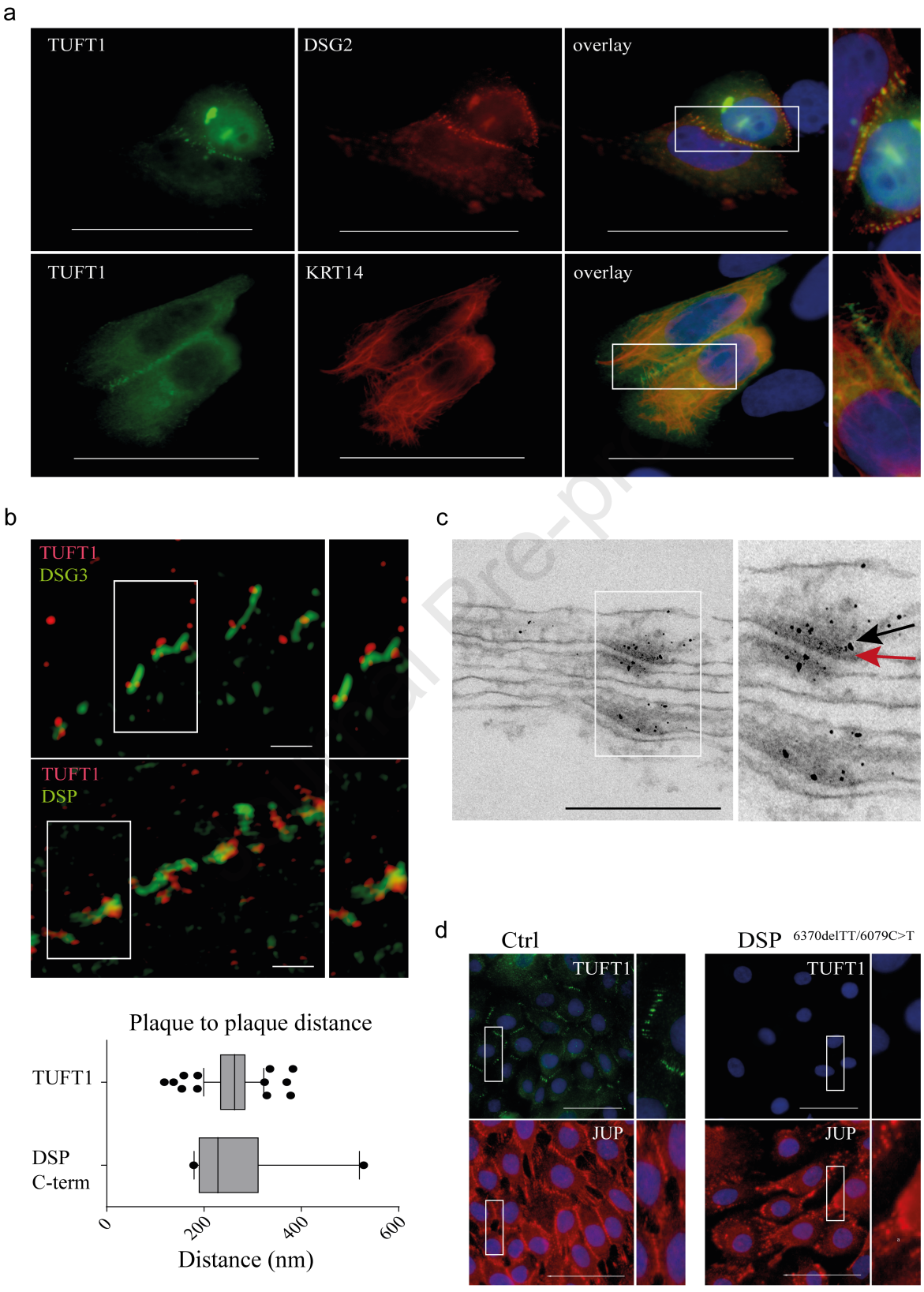
a
TUFT1
DSG2
overlay
TUFT1
KRT14
overlay
b
TUFT1
DSG3
TUFT1
DSP
Plaque to plaque distance
TUFT1
DSP
C-term
0
200
400
600
Distance (nm)
c
d
Ctrl
DSP 6370delTT/6079C>T
TUFT1
TUFT1
JUP
JUP

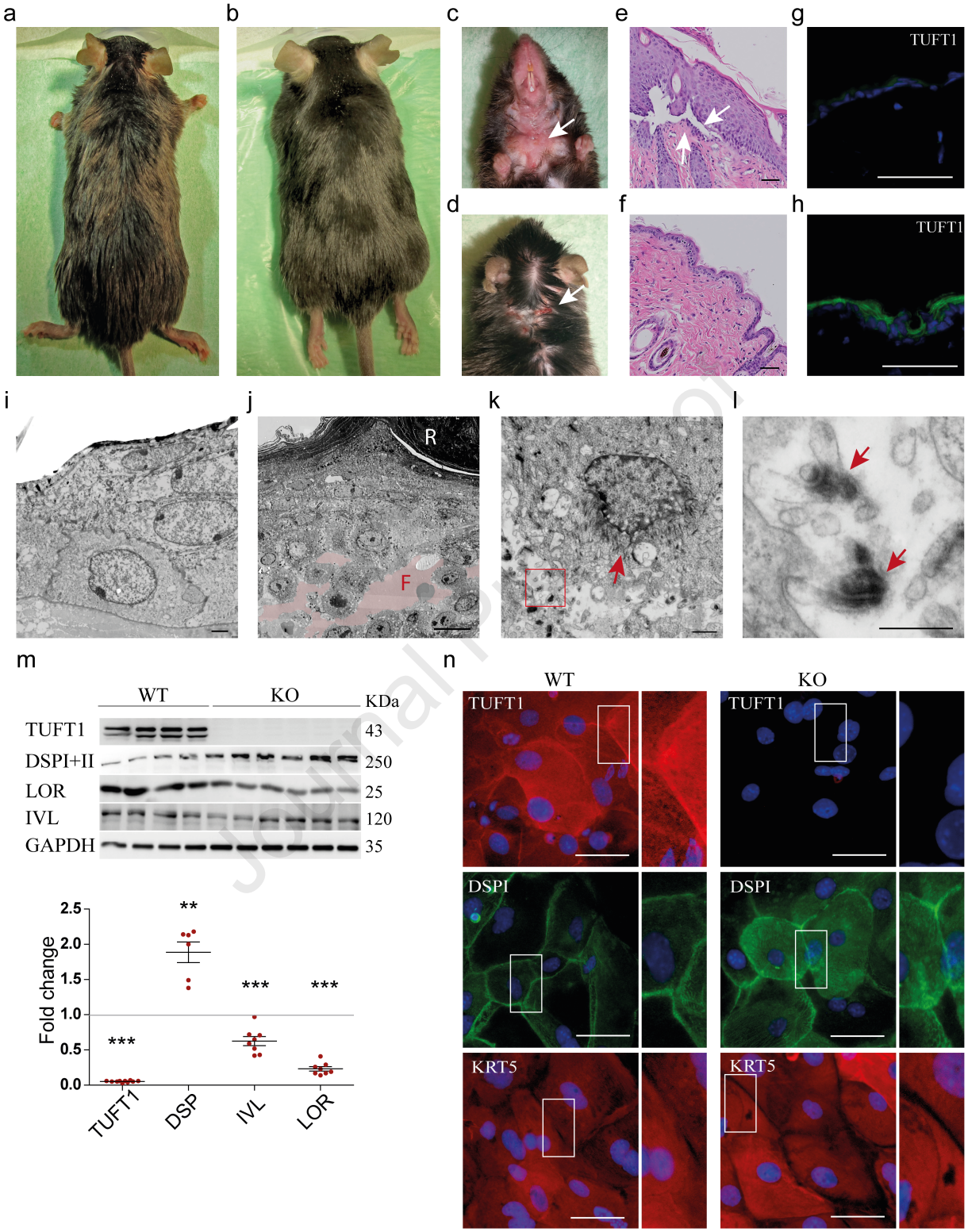
a
b
c
e
g
TUFT1
d
f
h
TUFT1
i
j
R
F
k
l
m
WT
KO
KDa
TUFT1
43
DSPI+II
250
LOR
25
IVL
120
GAPDH
35
Fold change
2.5
2.0
1.5
1.0
0.5
0.0
**
***
***
***
TUFT1
DSP
IVL
LOR
n
WT
KO
TUFT1
TUFT1
DSPI
DSPI
KRT5
KRT5